

Hydrogen adsorption in zeolites A, X, Y and RHO

H.W. Langmi^a, A. Walton^a, M.M. Al-Mamouri^a, S.R. Johnson^b, D. Book^{a,b}, J.D. Speight^a,
P.P. Edwards^{a,b}, I. Gameson^b, P.A. Anderson^b, I.R. Harris^{a,*}

^aDepartment of Metallurgy and Materials Science, School of Engineering, The University of Birmingham, Edgbaston, Birmingham B15 2TT, UK

^bSchool of Chemical Sciences, The University of Birmingham, Edgbaston, Birmingham B15 2TT, UK

Received 10 July 2002; received in revised form 13 September 2002; accepted 27 January 2003

Abstract

We have investigated the use of zeolites as potential hydrogen storage materials. The zeolites A, X, Y and RHO, which encompass a range of different pore geometries and compositions, were synthesised by hydrothermal methods, and different cation-exchanged forms were prepared through ion-exchange from aqueous metal nitrate solutions. The phase composition and crystallinity of samples were interrogated by powder X-ray diffraction. Scanning electron microscopy revealed cubic crystals of zeolites both before and after ion-exchange. Hydrogen adsorption capacities were measured using a constant pressure Thermogravimetric Analyser; data were obtained over a range of pressures from 0 to 15 bar and isothermally at temperatures from -196 to 300 °C. The results showed that hydrogen uptake in zeolites is strongly dependent upon temperature, and also on framework and cation type. Surface area measurements were also carried out on these materials and the results used to interpret the hydrogen adsorption data.

© 2003 Elsevier B.V. All rights reserved.

Keywords: Zeolites; Hydrogen adsorption

1. Introduction

Hydrogen storage is currently a topic of intensive research [1] because of the ever-growing environmental concerns over the use of fossil fuels. Various methods for storing hydrogen including gaseous, liquid and solid state storage have been suggested [1–3]. Recently, attention has focused on light materials such as carbon for solid-state hydrogen storage (see for example Refs. [4–6]). To date, only limited work has been carried out with regard to the hydrogen adsorption properties of other microporous materials such as zeolites despite the fact that the use of these materials for the separation of hydrocarbons and occlusion of gases is well established [7]. These applications have provided an early incentive for both theoretical [8] and experimental [9,10] studies on the adsorption of a range of gases (e.g. Ar, Xe, Kr, N₂) on zeolite materials. Of particular interest in relation to the potential use of these materials as gas storage media is that by changing the size and charge of the exchangeable cations, the diameter of the channels can be controlled, thus enabling the effective

trapping of different sized gas molecules. Weitkamp et al. [11] reported that sodalite could store $9.2 \text{ cm}^3/\text{g}$ (0.082 wt.%) of hydrogen if loaded at about 300 °C and 100 bar. At very low temperatures, hydrogen uptake values have been reported to be much higher. For instance, Kazansky et al. reported a study of hydrogen adsorption on sodium forms of faujasite and a hydrogen storage capacity of 3.6×10^{21} molecules/g (1.2 wt.%) at -196 °C [12].

In the present study we have carried out a systematic investigation of the hydrogen adsorption properties of a number of zeolites at three different temperatures. In order to examine a variety of framework structures, zeolites NaA (LTA structure type), NaX and NaY (FAU), and NaCsRHO (RHO)—and their ion-exchanged forms—have been chosen for study. The framework structures of these zeolites are shown in Fig. 1 and approximate pore sizes are given in Table 1.

2. Experimental

2.1. Hydrothermal preparation

Zeolite NaY was a commercial product obtained from Aldrich Chemical Company Inc. Zeolites NaA, NaX and

*Corresponding author. Tel.: +44-1214-145165; fax: +44-1214-145247.

E-mail address: i.r.harris@bham.ac.uk (I.R. Harris).

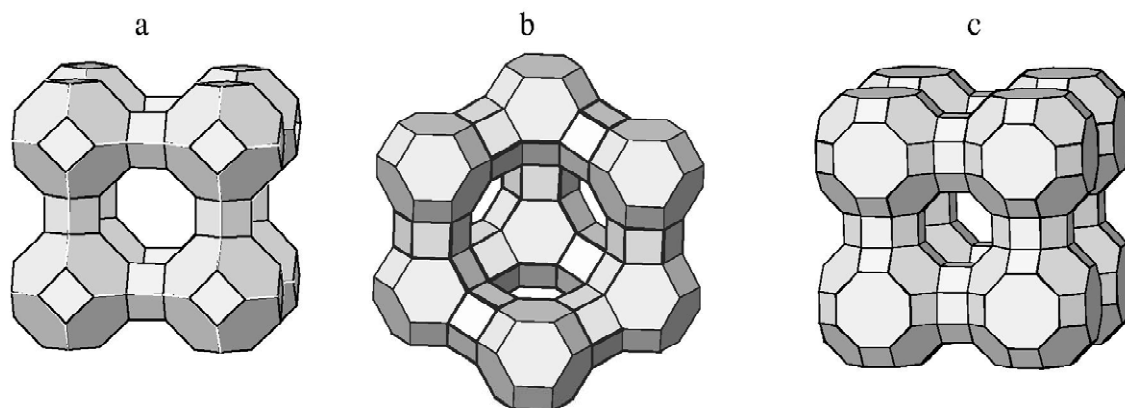


Fig. 1. Framework structures of zeolites: (a) zeolite A, (b) zeolites X and Y and (c) zeolite RHO. The corners on each framework represent Si or Al and these are linked by oxygen bridges represented by the lines on the frameworks (diagram kindly provided by M.J. Edmondson).

NaCsRHO were synthesized by three different hydrothermal routes. For a typical zeolite A synthesis, 2 g of sodium hydroxide (99% pellets, BDH), 24 g of sodium aluminate (99.9% Al, STREM Chemicals) and 46 g of sodium metasilicate (99%, STREM Chemicals) were used. Crystallization was carried out at 100 °C for 4 h in an oven.

NaX was prepared from solutions containing 60 g sodium metasilicate (99%, STREM Chemicals) and 19 g sodium aluminate (99.9% Al, STREM Chemicals). The two solutions were mixed together forming a thick gel, which was heated in an oven at 80 °C for 24 h.

For NaCsRHO, the preparation consisted of dissolving 36 g of sodium hydroxide (99% pellets, BDH) in deionized water, then adding 14 g alumina (Catapal B, Vista) to the resulting solution. The resulting solution was then added to 36 g of caesium hydroxide (50 wt.% with water, Aldrich) and 300 g colloidal silica (30 wt.% with water, Dupont Ludox HS-30). The gel was aged for 24 h at room temperature and then heated at 80 °C for 6 days. After reaction at the required temperature all samples were cooled, filtered, washed and dried to obtain zeolite crystals as a fine powder.

2.2. Ion exchange

Zeolites NaA, NaX, NaY and NaCsRHO were used as starting materials for ion-exchange. Exchange was carried out using conventional ion-exchange procedures. For Cd-exchanged zeolites, 10 g of the zeolite was added to 250 ml of 0.1 M $\text{Cd}(\text{NO}_3)_2$ (98%, Aldrich) solution at 70 °C

and stirred for 24 h. The exchange was performed five to seven times. In the case of Mg-exchanged zeolites, four exchanges were carried out at 80 °C using 100 ml of 0.4 M $\text{Mg}(\text{NO}_3)_2$ (99%, Aldrich) solution. These ions (Cd^{2+} and Mg^{2+}) were chosen as they have a higher charge than the native Na^+ cations, but have quite different sizes and chemistry, and because of their ability to be exchanged into a range of different zeolites without complication.

2.3. Characterization

The crystallinity of the zeolites was checked by means of powder X-ray diffraction (XRD) patterns obtained on a Siemens D5000 X-ray diffractometer with $\text{CuK}\alpha$ radiation. Morphological and compositional data were acquired through scanning electron microscopy (SEM) and energy dispersive X-ray (EDX) analysis respectively, using a JEOL 6300 electron microprobe. BET surface area measurements were performed on a Micromeritics ASAP 2010 machine using nitrogen adsorption at -196 °C. The hydrogen storage capacities of the zeolites were determined on a Hiden constant pressure Thermogravimetric Analyser, which is known as an Intelligent Gravimetric Analyser (IGA) system. Each sample, typically of mass 100 mg, was loaded into a glass sample bulb and the system evacuated (10^{-6} mbar) and heated to 400 °C to dry the samples. The samples were then cooled to the required temperature between -196 and 300 °C and, pressure–composition isotherms (PCT curves) determined up to 15 bar with 1 bar

Table 1
Approximate pore sizes of zeolites

Zeolite type	Type of cage	Diameter of cage (Å)	Free diameter of aperture (Å)
A	β	6.6	2.2
	α	11.4	4.1
X or Y	β	6.5	2.2
	supercage	11.8	7.4
RHO	α	11.0	3.6

pressure steps. The purity of the hydrogen source was 99.995%, and a liquid nitrogen trap was used on the hydrogen gas inlet stream. Results were corrected for buoyancy using Archimedes' Principle. Hydrogen adsorption values were expressed in terms of weight percent (wt.%) hydrogen in the material.

3. Results and discussion

X-ray diffraction patterns for zeolite Y samples are shown in Fig. 2. It can be seen clearly that the crystallinity of the zeolite framework was maintained after ion-exchange. SEM and XRD indicated that all the zeolites survived the ion-exchange procedures essentially intact (a significant reduction in peak intensities observed in CdY may result from sample absorption as the diffraction patterns were obtained in transmission mode). The estimated percentages of ion-exchange by EDX analysis were CdA, 87%; CdX, 100%; CdY, 100%; CdRHO, 57%; MgA, 78%; MgX, 73% and MgY, 59%.

The hydrogen uptake of all the zeolites was isothermally measured on the IGA at temperatures from RT to 300 °C up to a pressure of 15 bar. The largest uptake value between these temperatures was recorded at 270 °C and the highest hydrogen uptake at RT and 270 °C was recorded for NaA with values of 0.28 and 0.30 wt.%, respectively (Table 2). Weitkamp et al. [11] also observed higher hydrogen encapsulation at loading temperatures up to 300 °C. In the case of the current work the difference in uptake between RT and 270 °C could be due to experimental error, e.g. buoyancy or flow effects on the balance occurring at higher temperatures. Other workers have reported that higher uptakes can be achieved due to cationic vibrations at higher temperatures making the cages

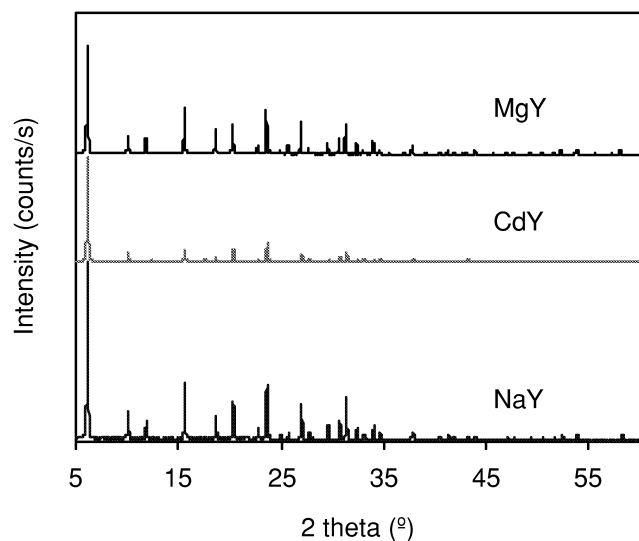


Fig. 2. Powder X-ray diffraction patterns of NaY, CdY and MgY zeolites.

Table 2

Hydrogen uptake (wt.%) in zeolites at pressure 15 bar and temperatures –196 °C, RT and 270 °C

Material	H ₂ uptake (wt.%)		
	–196 °C	RT	270 °C
NaA	1.54	0.28	0.30
CdA	1.14	0.25	0.30
MgA	1.19	N/A	N/A
NaCsRHO	0.00	0.18	0.20
CdRHO	0.08	0.19	0.25
NaX	1.79	N/A	0.25
CdX	1.42	N/A	N/A
MgX	1.61	N/A	0.28
CuX	N/A	N/A	0.25
NaY	1.81	N/A	N/A
CdY	1.47	N/A	N/A
MgY	1.74	N/A	N/A

more accessible [13]; it is not clear from the current work whether this phenomenon is indeed occurring.

Hydrogen uptake was substantially greater at –196 °C than at RT or 270 °C for zeolites A (Fig. 3), X (Fig. 4) and Y (Fig. 5). The hydrogen storage capacities obtained at –196 °C and 15 bar were 1.54, 1.79 and 1.81 wt.% for zeolites NaA, NaX and NaY, respectively. The results for NaX and NaY are in reasonable agreement with those of Kazansky et al. [12] who reported hydrogen uptake values of 1.2 wt.% at –196 °C and pressures <1 bar by barometric measurements and DRIFT spectra. For all the above mentioned zeolites adsorption/desorption traces were measured at liquid nitrogen temperature up to 2 bar with 0.1 bar pressure steps. An example (for CdA zeolite) is shown in Fig. 6. For all these zeolites, a Type I isotherm was observed, with desorption closely following the same path as adsorption: this indicates the process of microporous physisorption of hydrogen, as classified by Brunauer,

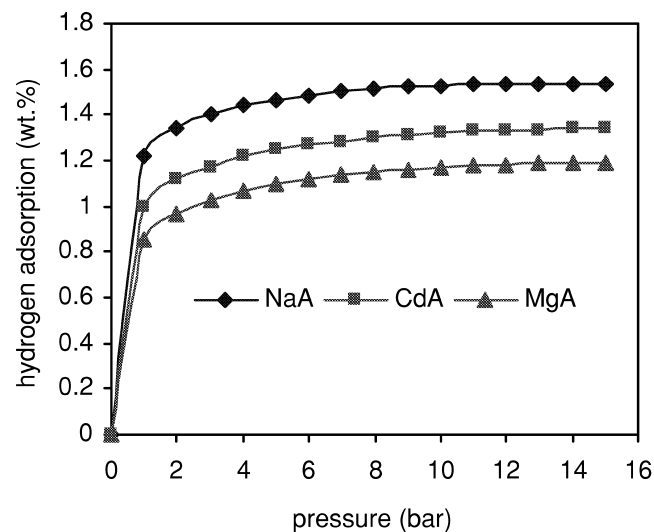


Fig. 3. Hydrogen adsorption isotherms at –196 °C for NaA, CdA and MgA zeolites with 1 bar pressure steps.

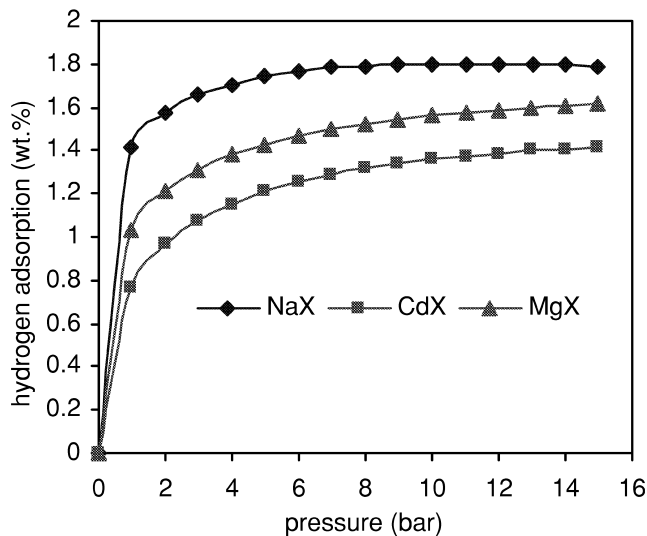


Fig. 4. Hydrogen adsorption isotherms at -196°C for NaX, CdX and MgX zeolites with 1 bar pressure steps.

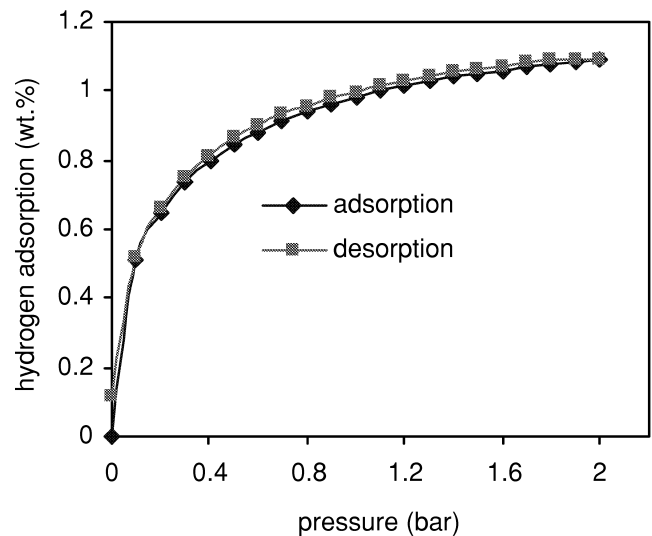


Fig. 6. Hydrogen adsorption/desorption isotherms at -196°C for CdA zeolite with 0.1 bar pressure steps.

Deming, Deming and Teller (BDDT) [14]. Zeolites have a characteristic high internal surface area, approximately of a similar order of magnitude to the surface area of activated carbon, a material which can exhibit appreciable hydrogen uptake values at cryogenic temperatures [15].

The influence of ion-exchange on hydrogen adsorption was investigated using Na, Cd and Mg forms of zeolites A, X and Y (Figs. 3, 4 and 5). Saturation was generally reached at higher pressures (5–9 bar) for zeolites X and Y in comparison to zeolite A, where adsorption became complete at pressures of 3–5 bar. Hydrogen adsorption decreased from Na^{+} through Mg^{2+} to Cd^{2+} in zeolites X

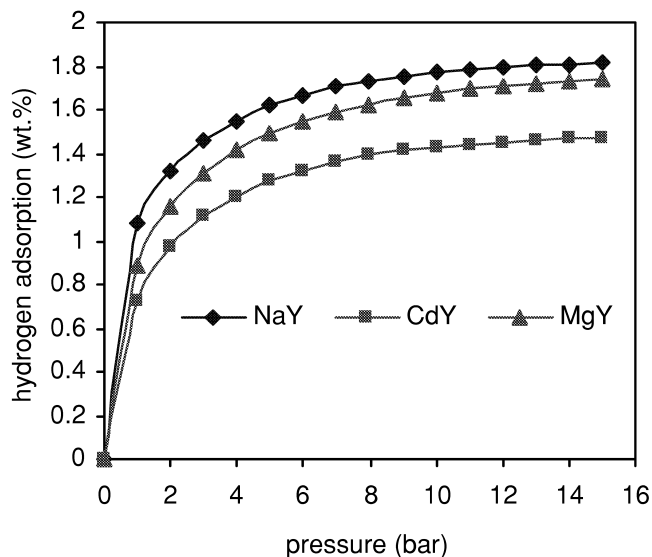


Fig. 5. Hydrogen adsorption isotherms at -196°C for NaY, CdY and MgY zeolites with 1 bar pressure steps.

(Fig. 4) and Y (Fig. 5) although we note that there are differences in measured ion-exchange capacities for the various cationic forms.

Fraenkel [8] postulated that hydrogen uptake in zeolites was related directly to the available void volume per gram of zeolite which decreases with the increasing size and number of the exchangeable cations. From our data, this explanation does not appear to hold for zeolites X, Y and A, where, for instance, NaX and NaY have twice as many—and larger—cations than MgX and MgY, yet the uptake was lower for the Mg-exchanged zeolites. As zeolites X and Y have very open structures it is unlikely that the lower uptake observed for ion-exchanged X and Y is due to a cationic ‘pore blocking’ effect. It is possible that a small amount of structural imperfection (not detected by XRD or SEM) may be responsible for the lower uptakes—effectively blocking entry points to the crystallite, or alternatively that the association of molecular hydrogen with the metal cation itself has a large effect on the physisorption values.

Zeolite A followed a similar trend in hydrogen uptake values as X and Y for Na- and Mg-exchanged forms, despite the fact that this zeolite has a significantly different crystal structure (Fig. 1). It might have been expected that CdA and MgA would have had a higher uptake in comparison to that of NaA, as Cd^{2+} and Mg^{2+} probably sit in the 6-ring sites of the α -cages leaving the larger 8-ring sites accessible to hydrogen. Sodium occupies both the 6-ring sites and the larger 8-ring openings.

Interestingly, the amount of hydrogen adsorption by zeolite RHO at liquid nitrogen temperatures was insignificant (Fig. 7). A possible reason for the low uptake in NaCsRHO at this cryogenic temperature is the fact that access to this structure might be effectively blocked by

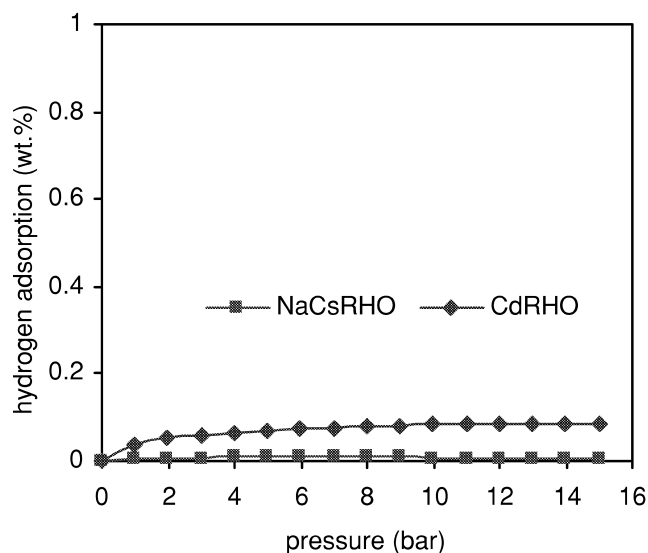


Fig. 7. Hydrogen adsorption isotherms at $-196\text{ }^{\circ}\text{C}$ for NaCsRHO and CdRHO zeolites with 1 bar pressure steps.

Cs^+ cations which are located in the double 8-ring sites. EDX analysis revealed that Cs^+ ions were still present in the Cd-exchanged zeolite RHO. Therefore, either there are enough Cs^+ cations left in CdRHO after ion-exchange to prevent significant hydrogen uptake, or the Cd^{2+} cation in zeolite RHO itself exerts a blocking effect. The local positioning of these cations in zeolite RHO structures has been reported as an important parameter for the encapsulation of hydrogen gas molecules [13].

The large internal surface area of the zeolite structures plays a major role in the relatively high hydrogen/adsorption values observed [15]. BET measurements (using nitrogen) were carried out in order to compare hydrogen uptake to total surface area. BET values have previously been shown to relate closely to micropore volumes in zeolite materials [15]. The observed trend in the BET measurements (Table 3) followed the order $\text{NaY} > \text{NaX} > \text{CdY} > \text{CdX} > \text{CdA} > \text{CdRHO} > \text{NaCsRHO}$. The data for NaA however, are not included in Table 3 because a very small nitrogen sorption capacity was obtained and hence the BET surface area could not be reliably estimated [16].

The BET surface area was plotted against hydrogen

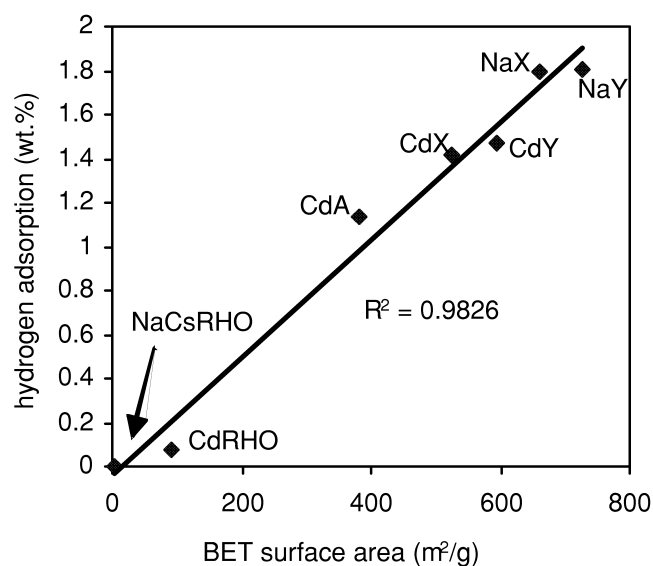


Fig. 8. Correlation between hydrogen adsorption at $-196\text{ }^{\circ}\text{C}$ and BET surface area for a series of zeolite materials. The correlation coefficient is also indicated.

uptake values for all systems investigated (Fig. 8) and it can be seen that the hydrogen uptake correlates directly with the measured BET surface area. One exception is NaA which takes up 1.54 wt.% hydrogen at liquid nitrogen temperatures yet has an immeasurably low BET surface area. This is probably due to the smaller size of the hydrogen molecule in comparison to that of nitrogen and to the size of the pore opening. As expected, NaCsRHO and CdRHO gave a low BET surface area due to pore blocking by the large cations. In future, more sophisticated Dubinin-type analyses [14] will be carried out on both the nitrogen and hydrogen isotherms at $-196\text{ }^{\circ}\text{C}$.

4. Conclusions

The largest hydrogen uptake values for zeolites A, X and Y were found to be at $-196\text{ }^{\circ}\text{C}$. The fact that hydrogen uptake was of a Type I nature (desorption followed the same path as adsorption on the PCT plots) proved that, at low temperatures at least, microporous adsorption was the dominant mechanism. Ion exchange has been shown to have an effect on the hydrogen adsorption values at $-196\text{ }^{\circ}\text{C}$, however, it is not yet clear whether the observed differences in adsorption values are due to pore blocking by cations, or variations in the interaction of hydrogen with different cations. Further work is required to understand fully these mechanisms. A maximum hydrogen storage capacity of 1.81 wt.% (at $-196\text{ }^{\circ}\text{C}$ and 15 bar) was observed for NaY zeolite. These materials show great promise/potential as low cost media for stationary hydrogen storage applications.

Table 3
BET surface area (m^2/g) of zeolites

Material	BET surface area (m^2/g)
NaA	N/A
CdA	383
NaCsRHO	3
CdRHO	90
NaX	622
CdX	526
NaY	725
CdY	594

Acknowledgements

Thanks are due to Overseas Research Student Award Scheme/School of Engineering for providing funding to HWL. We also acknowledge the *EU Fuel Cell and Hydrogen Store for Integration into Automobiles* (FUCH-SIA) project, part of the Framework 5 Energie Programme.

References

- [1] L. Schlapbach, MRS Bull. 12 (2002) 675.
- [2] S.M. Aceves, G.D. Berry, G.D. Rambach, Int. J. Hydrogen Energy 23 (1998) 583.
- [3] K.D. Chung, M.S. Lee, O.S. Joo, S.H. Han, S.J. Uhm, in: T.O. Saetre (Ed.), Hydrogen Power: Theoretical and Engineering Solutions, Kluwer Academic Publishers, Netherlands, 1998, pp. 43–48.
- [4] M.S. Dresselhaus, K.A. Williams, P.C. Eklund, MRS Bull. 24 (1999) 45.
- [5] A.C. Dillon, M.J. Heben, Appl. Phys. A 72 (2001) 133.
- [6] A. Züttel, Ch. Nützenadel, P. Sudan, Ph. Mauron, Ch. Emmenegger, S. Rentsch, L. Schlapbach, A. Weidenkaff, T. Kiyobayashi, J. Alloys Comp. 330–332 (2002) 676.
- [7] R.M. Barrer, Zeolites and Clay Minerals as Sorbents and Molecular Sieves, Academic Press, London, 1978.
- [8] D. Fraenkel, J. Chem. Soc. Faraday Trans. 1 (77) (1981) 2041.
- [9] D.R. Corbin, L. Abrams, G.A. Tones, M.L. Smith, C.R. Dybocski, J.A. Hriljac, J.B. Parise, J. Chem. Soc., Chem. Commun. 12 (1993) 1027.
- [10] S. Bordiga, G.T. Palomino, C. Pazè, A. Zecchina, Microporous Mesoporous Mater. 34 (2000) 67.
- [11] J. Weitkamp, M. Fritz, S. Ernst, Int. J. Hydrogen Energy 20 (1995) 967.
- [12] V.B. Kazansky, V.Y. Borovkov, A. Serich, H.G. Karge, Microporous Mesoporous Mater. 22 (1998) 251.
- [13] V.V. Krishnan, S.L. Suib, D.R. Corbin, S. Schwarz, G.E. Jones, Catal. Today 31 (1996) 199.
- [14] S.J. Gregg, K.S.W. Sing, Adsorption, Surface Area and Porosity, 2nd Edition, Academic Press, London, 1982, Chapter 4.
- [15] M.G. Nijkamp, J.E.M.J. Raaymakers, A.J. van Dillen, K.P. de Jong, Appl. Phys. A 72 (2001) 619.
- [16] P.A. Zielinski, A.V. Neste, D.B. Akolekar, S. Kaliaguine, Microporous Mater. 5 (1995) 123.